Journal of Catalysis 282 (2011) iii–ix

Contents lists available at ScienceDirect

Journal of Catalysis

journal homepage: www.elsevier.com/locate/jcat

Journal of Catalysis Vol. 282, Issue 1, 2011

Contents

Easy synthesis of three-dimensionally ordered macroporous $La_{1-x}K_xCoO_3$ catalysts and their high activities for the catalytic combustion of soot **pp 1–12**

Junfeng Xu, Jian Liu, Zhen Zhao*, Chunming Xu, Jianxiong Zheng, Aijun Duan, Guiyuan Jiang

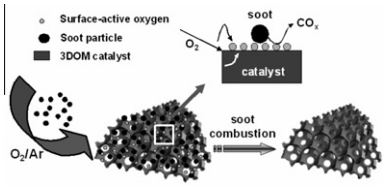

The three-dimensionally ordered macroporous perovskite $La_{1-x}K_xCoO_3$, prepared using a novel carboxy-modified colloidal crystal template, shows excellent performance in catalytic for soot combustion.

Kinetic studies of the stability of Pt for NO oxidation: Effect of sulfur and long-term aging **pp 13–24**

Jorge H. Pazmiño, Jeffrey T. Miller, Shadab S. Mulla, W. Nicholas Delgass, Fabio H. Ribeiro*

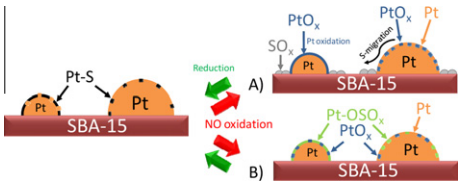

Two pathways are suggested during NO oxidation: (A) sulfur migration to interfacial support sites driven by the oxidation of surface Pt and (B) formation of Pt–OSO_x followed by Pt oxidation. In both cases, the number of Pt sites that overcome sulfidation and/or oxidation is the same as for the S-free catalyst.

Effect of nanosize on catalytic properties of ferric (hydr)oxides in water: Mechanistic insights **pp 25–34**

Irina V. Chernyshova*, Sathish Ponnurangam, Ponisseril Somasundaran

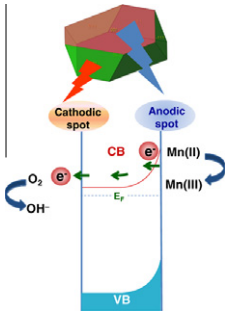

A decrease in the Mn(II) oxygenation rate on hematite and ferrihydrite nanoparticles with decreasing particle size is explained by the electrochemical route of the reaction.

Effect of pretreatment on precipitated Fe–Mo Fischer–Tropsch catalysts: Morphology, carburization, and catalytic performance pp 35–46

Xiaojing Cui, Jian Xu*, Chenghua Zhang, Yong Yang, Peng Gao, Baoshan Wu, Yongwang Li*

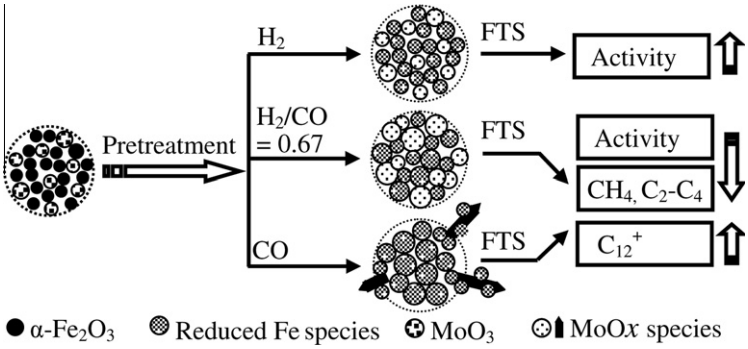

Pretreatment induced migrations of Mo affect the size distribution and local environments of iron active sites.

Exploring the void structure and activity of RUB-39 based expanded materials using the hydroconversion of decane pp 47–53

Bart Tijsebaert, Mathieu Henry, Hermann Gies, Feng-Shou Xiao, Weiping Zhang, Xinhe Bao, Hiroyuki Imai, Takashi Tatsumi, Ulrich Müller, Bilge Yilmaz, Pierre Jacobs, Dirk De Vos*

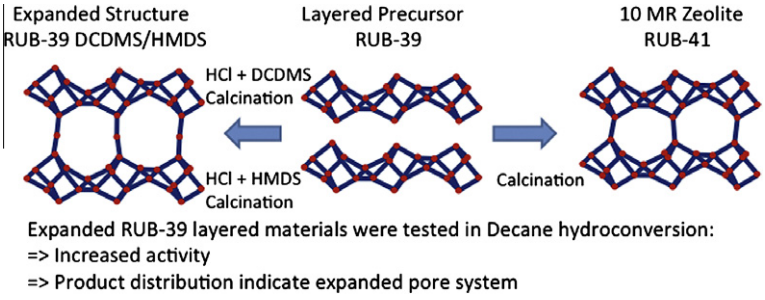

Starting from the layered precursor RUB-39, a interlayer expanded material containing Al is prepared. The results of the decane hydrocracking prove that the pores are effectively expanded in comparison with the related zeolite RUB-41.

Oxidative dehydrogenation of a biomass derived lignan – Hydroxymatairesinol over heterogeneous gold catalysts pp 54–64

Olga A. Simakova, Elena V. Murzina, Päivi Mäki-Arvela, Anne-Riikka Leino, Betiana C. Campo, Krisztián Kordás, Stefan M. Willför, Tapio Salmi, Dmitry Yu. Murzin*

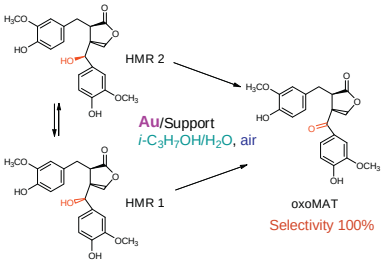

Synthesis of lignan oxomatairesinol (oxoMAT) via oxidative dehydrogenation of the naturally occurring lignan hydroxymatairesinol (HMR), which exists in nature as a mixture of two diastereomers: (7R,8R,8'R)-(-)-7-allo-hydroxymatairesinol and (7S,8R,8'R)-(-)-7-allo-hydroxymatairesinol, was studied over supported gold catalysts. Applying gold catalysts boosts the selectivity toward oxomatairesinol up to 100%.

Asymmetric epoxidation of chalcone catalyzed by reusable poly-L-leucine immobilized on hydrotalcite pp 65–73

Ronald-Alexander Miranda, Jordi Llorca, Francisco Medina, Jesús E. Sueiras, Anna M. Segarra*

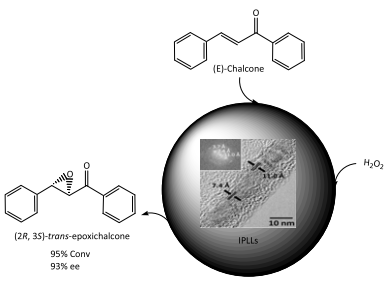

Highly active and recyclables nanohybrid synzymes for asymmetric epoxidation reaction.

C–H bond activation of methane on clean and oxygen pre-covered metals: A systematic theoretical study **pp 74–82**
Bin Xing, Xian-Yong Pang, Gui-Chang Wang*

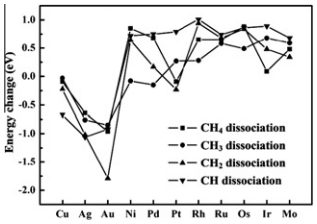

Density functional calculations indicate that pre-adsorbed oxygen on noble metal surfaces promotes methane dissociation, while it inhibits this process on transition metal surfaces.

Reactivity and in situ X-ray absorption spectroscopy of Rb-promoted Mo_2C/MgO catalysts for higher alcohol synthesis **pp 83–93**
Heng Shou, Robert J. Davis*

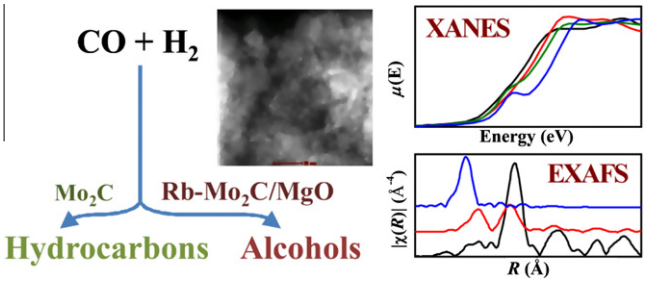

Nanoparticles of Mo_2C were supported on MgO, extensively characterized by a variety of methods, and evaluated as catalysts for syngas conversion to alcohols. Addition of Rb_2CO_3 promoted the alcohol synthesis reaction at the expense of hydrocarbon formation. Since bulk Mo_2C was primarily a Fischer–Tropsch catalyst, the basic support and the promoter are critical components for alcohol synthesis.

Au/TiO_2@SBA-15 nanocomposites as catalysts for direct propylene epoxidation with O_2 and H_2 mixtures **pp 94–102**
Chun-Hsia Liu, Yejun Guan, Emiel J.M. Hensen, Jyh-Fu Lee, Chia-Min Yang*

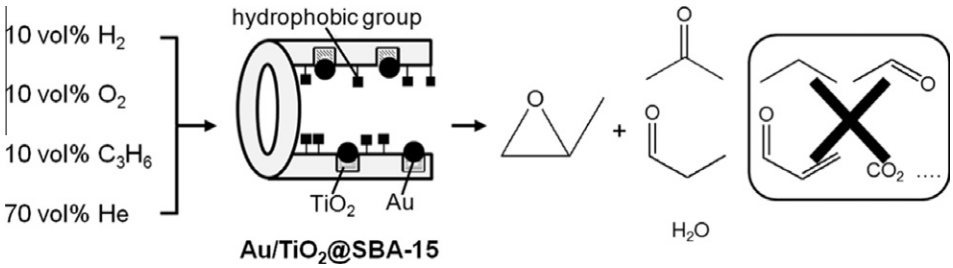

Small Au nanoparticles in close contact with nanosized TiO_2 selectively embedded in the micropores of SBA-15 show high stability in the direct epoxidation of propylene with O_2/H_2 mixture and produce propylene oxide with only propanal and acetone as minor byproducts.

Deactivation and regeneration studies of a PdSb/TiO_2 catalyst used in the gas-phase acetoxylation of toluene **pp 103–111**
N. Madaan, S. Gatla, V.N. Kalevaru, J. Radnik, B. Lücke, A. Brückner, A. Martin*

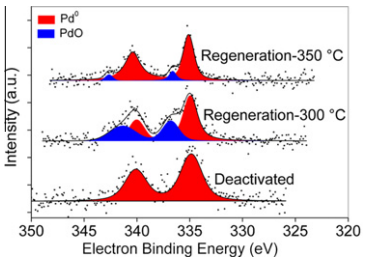

A PdSb/titania catalyst showed significant deactivation after 33 h on-stream. The deactivation is due to coking and a loss of PdO surface species. The deactivated catalyst was regenerated at 250–400 °C for 2 h in air. The deactivation is reversible with respect to coke but irreversible at higher regeneration temperatures (>350 °C) concerning the PdO surface proportion as revealed by XPS.

Supported L-proline on zirconium phosphates methyl and/or phenyl phosphonates as heterogeneous organocatalysts for direct asymmetric aldol addition pp 112–119

Salvatore Calogero, Daniela Lanari, Mara Orrù, Oriana Piermatti*, Ferdinando Pizzo, Luigi Vaccaro

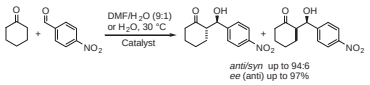

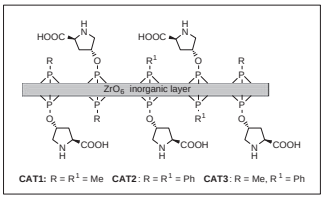

Zirconium phosphates methyl and/or phenyl phosphonates-supported L-proline have been prepared as amorphous solids and their catalytic activity tested on the direct asymmetric aldol addition of cyclohexanone to *p*-nitrobenzaldehyde in DMF/H_2O (9:1) and in sole water.

Palladium-catalyzed synthesis of symmetrical urea derivatives by oxidative carbonylation of primary amines in carbon dioxide medium pp 120–127

Nicola Della Ca', Paolo Bottarelli, Angela Dibenedetto, Michele Aresta, Bartolo Gabriele, Giuseppe Salerno, Mirco Costa*

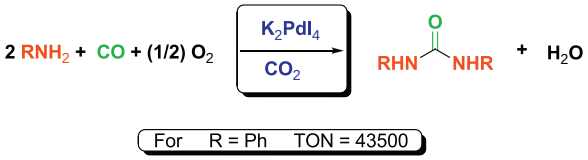

Primary aliphatic and aromatic amines and carbon monoxide react effectively in solvent-free conditions and/or in carbon dioxide medium in the presence of tetraiodopalladate and oxygen leading to symmetrical urea derivatives. The use of carbon dioxide as the solvent medium allows in some cases high performance of the catalyst in terms of turnover number.

Catalytic behaviour of hybrid LNT/SCR systems: Reactivity and in situ FTIR study pp 128–144

L. Castoldi, R. Bonzi, L. Lietti, P. Forzatti*, S. Morandi, G. Ghiotti, S. Dzwigaj

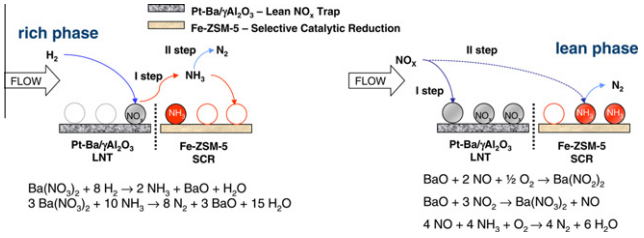

In the LNT/SCR dual bed during the rich phase the reduction of NO_x stored onto LNT catalyst gives NH_3 (I step) and then N_2 (II step). NH_3 slipped from LNT catalyst is adsorbed onto SCR catalyst. In the lean phase NO_x are stored onto LNT catalyst (I step) and react with NH_3 adsorbed onto SCR catalyst via SCR reaction (II step). This lowers the ammonia slip and increases the NO_x removal efficiency. The LNT/SCR physical mixture also shows a NO_x removal efficiency higher than the single LNT catalyst.

Hydrocracking reaction pathways of 2,6,10,14-tetramethylpentadecane model molecule on bifunctional silica–alumina and ultrastable Y zeolite catalysts pp 145–154

G. Burnens, C. Bouchy, E. Guillon, J.A. Martens*

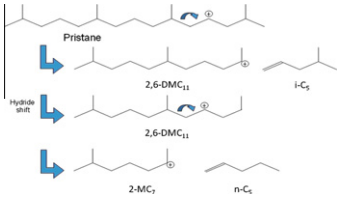

Hydrocracking modes of pristane (2,6,10,14-tetramethylpentadecane) reveal the need of a paradigm shift to cope with hydrocracking mechanisms of renewable hydrocarbon feedstock.

Effect of water on the stability of Mo and CoMo hydrodeoxygenation catalysts: A combined experimental and DFT study **pp 155–164**
M. Badawi, J.F. Paul, S. Cristol, E. Payen, Y. Romero, F. Richard, S. Brunet, D. Lambert, X. Portier, A. Popov, E. Kondratieva, J.M. Goupil, J. El Fallah, J.P. Gilson, L. Mariey, A. Travert*, F. Maugé

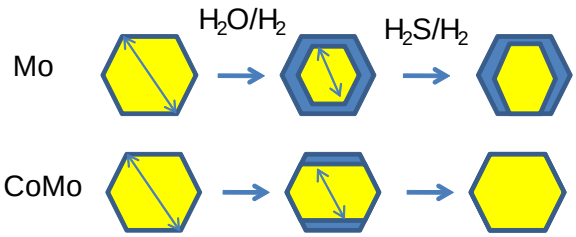

Water impacts the stability of Mo and CoMo sulfide catalysts in hydrodeoxygenation of phenolic compounds. Co promotes the catalytic activity and stabilizes the active phase in the presence of water.

Novel Pt/Mg(In)(Al)O catalysts for ethane and propane dehydrogenation **pp 165–174**
Pingping Sun, Georges Siddiqi, William C. Vining, Miaofang Chi, Alexis T. Bell*

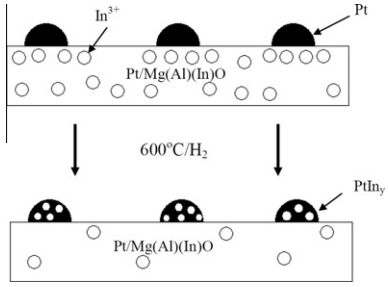

PtIn bimetallic catalysts have been prepared by depositing Pt nanoparticles on the surface hydrotalcite-like supports, Mg(In)(Al)O. These catalysts are highly active and selective for the dehydrogenation of ethane and propane to ethene and propene, respectively.

Highly selective metal fluoride catalysts for the dehydrohalogenation of 3-chloro-1,1,1,3-tetrafluorobutane **pp 175–182**
Katharina Teinz, Stefan Wuttke, Fabian Börno, Johannes Eicher, Erhard Kemnitz*

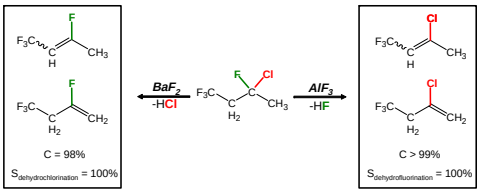

Using nanoscopic metal fluorides as catalysts, 3-chloro-1,1,1,3-tetrafluorobutane can be selectively converted into the respective olefins by either AlF3 (dehydrofluorination, $X > 99\%$, $S = 100\%$) or BaF2 (dehydrochlorination, $X = 98\%$, $S = 100\%$). A mechanistic rationalization is presented.

Oxygen reduction reaction mechanism on nitrogen-doped graphene: A density functional theory study **pp 183–190**
Liang Yu, Xiulian Pan, Xiaoming Cao, P. Hu*, Xinhe Bao*

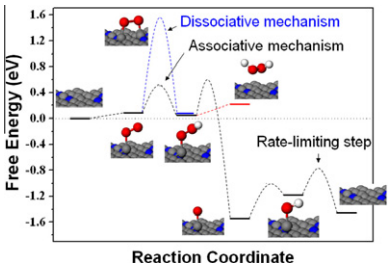

The electrocatalytic reduction of oxygen on nitrogen-doped graphene in alkaline solution follows an associative mechanism which is energetically more favorable than the dissociative mechanism. The rate-limiting step of the reaction is the $O_{(ads)}$ removal from the surface. The formation of peroxide is energetically unfavored.

Direct oxidation of methanol to formaldehyde by N_2O on $[Fe]^{1+}$ and $[FeO]^{1+}$ sites in Fe–ZSM-5 zeolite: A density functional theory study pp 191–200
Mehmet Ferdi Fellah

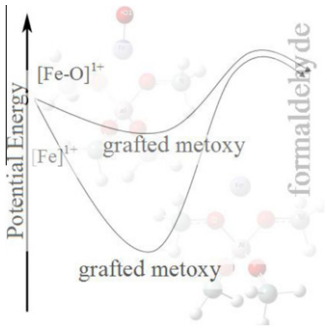

Density functional theory calculations indicated that $[Fe–O]^{1+}$ site in Fe–ZSM–5 catalyst has a positive role on the catalytic direct oxidation of methanol to formaldehyde by N_2O.

Oxidative desulfurization (ODS) of organosulfur compounds catalyzed by peroxo-metallate complexes of WO*x*–ZrO_2: Thermochemical, structural, and reactivity indexes analyses pp 201–208
E. Torres-García*, A. Galano*, G. Rodriguez-Gattorno

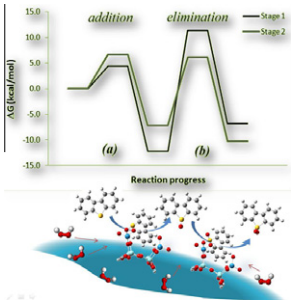

The experimental-theoretical study reveal that the oxidative desulfurization (ODS) process takes place in two stages, the formation of sulfoxide and the formation of sulfone and that each stage occur in two independent steps, addition (*1a* and *2a*) and elimination (*1b* and *2b*), involving the formation of intermediate adducts. The values of the Gibbs free energy of activation show that the barriers of the addition steps are significantly lower than those of the elimination steps, supporting the hypothesis that the elimination is the rate-determining step of the ODS process.

Aerobic oxidation of monoterpenic alcohols catalyzed by ruthenium hydroxide supported on silica-coated magnetic nanoparticles pp 209–214
Vinícius V. Costa, Marcos J. Jacinto, Liane M. Rossi, Richard Landers, Elena V. Gusevskaya*

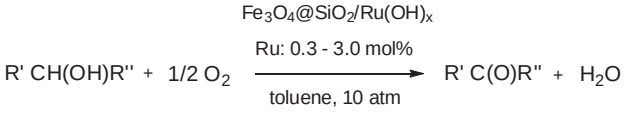

A magnetic material comprised of ruthenium hydroxide supported on silica-coated Fe_3O_4 nanoparticles is an effective catalyst for the liquid-phase aerobic oxidation of a wide range of alcohols into corresponding aldehydes and ketones. The oxidation of biomass-based monoterpenic alcohols gives carbonylic terpenoids useful for fragrance and pharmaceutical industries.

Control of surface acidity and catalytic activity of γ-Al_2O_3 by adjusting the nanocrystalline contact interface pp 215–227
Roxana Vidruk, Miron V. Landau*, Moti Herskowitz, Vladimir Ezersky, Amir Goldbourt

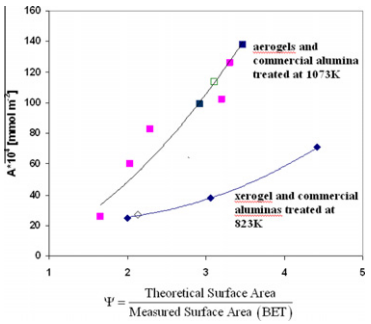

Increasing the nanocrystals contact interface in γ-alumina reflected by the increase in crystals aggregation ratio Ψ enhances its surface acidity in spite of decreasing the surface area.

Influence of the support composition and acidity on the catalytic properties of mesoporous SBA-15, Al-SBA-15, and Al_2O_3-supported Pt catalysts for cinnamaldehyde hydrogenation **pp 228–236**

Soraya Handjani, Eric Marceau*, Juliette Blanchard, Jean-Marc Krafft, Michel Che, Päivi Mäki-Arvela, Narendra Kumar, Johan Wärnå, Dmitry Yu. Murzin

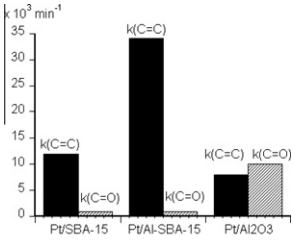

In liquid phase, the hydrogenation of the cinnamaldehyde C=C bond is favored on Pt/SBA-15 and Pt/Al-SBA-15, but reaction rates are significantly higher on the latter catalyst. In contrast, on mesoporous Pt/Al_2O_3, C=C and C=O hydrogenations take place at the same rate. When metal particles are small enough (<2 nm), the composition and acidity of the support influence the particles adsorptive properties as well as the reaction rate and selectivity.

Liquid-phase glycerol hydrogenolysis to 1,2-propanediol under nitrogen pressure using 2-propanol as hydrogen source **pp 237–247**

I. Gandarias*, P.L. Arias, J. Requies, M. El Doukkali, M.B. Güemez

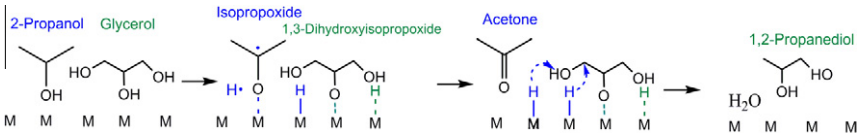

Proposed reaction pathway through alkoxide formation for glycerol hydrogenolysis to yield 1,2-propanediol under N_2 pressure using 2-propanol as a hydrogen donor molecule.